



Published in final edited form as:

Nat Struct Mol Biol. 2009 September ; 16(9): 973–978. doi:10.1038/nsmb.1643.

Molecular mechanisms for protein-encoded inheritance

Jed J. W. Wiltzius¹, Meytal Landau¹, Rebecca Nelson¹, Michael R. Sawaya¹, Marcin I. Apostol¹, Lukasz Goldschmidt¹, Angela B. Soriaga¹, Duilio Cascio¹, Kanagalaghatta Rajashankar², and David Eisenberg¹

¹UCLA-DOE Institute for Genomics and Proteomics, Howard Hughes Medical Institute, Molecular Biology Institute, UCLA, Box 951570, Los Angeles CA 90095-1570, USA

²NE-CAT and Dept. of Chemistry and Chemical Biology, Cornell University, Building 436E, Argonne National Laboratory, 9700 S. Cass Avenue, Argonne, IL 60439

Abstract

Strains are phenotypic variants, encoded by nucleic acid sequences in chromosomal inheritance and by protein “conformations” in prion inheritance and transmission. But how is a protein “conformation” stable enough to endure transmission between cells or organisms? Here new polymorphic crystal structures of segments of prion and other amyloid proteins offer structural mechanisms for prion strains. In *packing polymorphism*, prion strains are encoded by alternative packings (polymorphs) of β -sheets formed by the same segment of a protein; in a second mechanism, *segmental polymorphism*, prion strains are encoded by distinct β -sheets built from different segments of a protein. Both forms of polymorphism can produce enduring “conformations,” capable of encoding strains. These molecular mechanisms for transfer of information into prion strains share features with the familiar mechanism for transfer of information by nucleic acid inheritance, including sequence specificity and recognition by non-covalent bonds.

Introduction

Prions are infectious proteins that, in mammals, give rise to transmissible neurodegenerative diseases¹ and, in fungi, produce heritable and sometimes beneficial phenotypes^{2, 3}. Although distinctly different in sequence and cellular role, the mammalian and most fungal prion proteins share similarities in their mechanisms of prion formation and propagation^{2, 4}. Prion formation involves a structural conversion, in which the protein changes from its normal, soluble structure to an aggregated, amyloid-like structure rich in β -sheets. This conversion involves breaking intramolecular non-covalent bonds and forming intermolecular hydrogen-bonds and other non-covalent bonds. The resulting prion aggregates then seed the conversion of identical soluble protein molecules to the aggregated state. Mammalian and fungal prions also share the phenomenon of strains, in which structural conversions of the same protein give rise to different disease characteristics or phenotypes². While mammalian disease strains show a correlation with differences in prion conformation^{5–7}, the causal link

Correspondence should be addressed to: david@mbi.ucla.edu, Phone: +310 825-3754. Fax: +310 206-3914.

Note: Supplementary information is available on the Nature Structural & Molecular Biology website.

Database accession numbers: The coordinates and structure factors have been deposited in the Protein Data Bank (accession codes: 3FVA (NNQNTF), 3FQP (VQIVYK Form 2), 3FR1 (NFLVHS), 3FTH (NFLVHSS), 3FPO (HSSNNF), 3FOD (AILSST), 3FTR (SSTNVG Form 2), 3FTK (NVGSNTY Form 1) and 3FTL (NVGSNTY Form 2).

AUTHOR CONTRIBUTIONS

J.J.W.W., M.L., R.N., M.R.S. planned, executed, analyzed research and coauthored paper; L.G. planned and analyzed research; A.S. executed and analyzed research; D.C. and R.K. collected X-ray diffraction data; D.E. supervised research and coauthored paper.

has been proven in yeast – distinct conformations of aggregated Sup35 give rise to distinct strains of $[PSI^+]$ ^{8,9}.

Amyloid fibrils, though not generally infectious, share with prion aggregates their cross- β spine structure and a propensity for conformational variation, or *polymorphism*. Amyloid conformers give rise to fibrils with distinct properties, such as NMR spectra¹⁰ and morphology^{10, 11} – for example, twisted versus flat fibrils, or fibrils of different widths. Similar morphologies have been observed for in vitro-formed mammalian prion fibrils¹², suggesting commonalities between the conformational differences that produce amyloid fibril polymorphism and those that give rise to prion strains. The observation that an amyloid disease is transmissible in mice¹³ further blurs the distinction between amyloid and prion.

Despite pioneering studies^{14–19}, little is known at the atomic level about the nature of the conformational differences that give rise to polymorphic amyloid fibrils and prion strains. In our previous work, we determined thirteen fibril-like structures of segments from proteins known to fibrillize; these structures consisted of pairs of tightly packed, highly complementary β -sheets^{20, 21} which we termed *steric zippers*. Each steric zipper is formed from identical short segments of protein molecules, stacked into β -sheets that run the entire length of the amyloid-like fibrils, and of the closely-related needle-shaped microcrystals^{21, 22} used to determine the atomic structures of the steric zippers. We noted that these steric zippers included three polymorphic pairs (alternative packings) which might be connected to the phenomenon of prion strains. Since then, in the course of determining new fibril-like structures, we have found that polymorphic structures are common among steric zippers. Here we present nine new structures that include three distinct types of steric zippers, and present the structural and biochemical arguments that indicate the conformational differences of prion strains may be attributable to polymorphic steric-zippers. We also discuss the similarities in information transfer between protein-encoded prion inheritance, and the more familiar nucleic acid-encoded inheritance.

RESULTS

Packing polymorphism of steric zippers

In determining the atomic structures of steric zippers by X-ray microcrystallography, including nine new structures reported here (Tables 1, 2, and Supplementary Table 1), we have found that some segments of amyloid and prion proteins form two packing types, or *polymorphs*. Four such pairs are shown in Figure 1. The fibril-forming segment²² SSTNVG is derived from islet amyloid polypeptide (IAPP), a 37-residue hormone that forms fibrillar amyloid deposits among the pancreatic β -islet cells of nearly all type II diabetics²³. Microcrystals of SSTNVG grown from different solutions revealed two structures (polymorphs), one featuring a pair of serine residues at the center (Fig. 1a, left)²² and the other, with a shifted registration of the two β -sheets, featuring a pair of asparagine residues at the center (Fig. 1a, right). In both polymorphs, a pair of tightly interdigitated β -sheets, with no water molecules in the interface, forms the basic dry steric zipper structure. A second pair of polymorphic steric zippers is formed by the segment VQIVYK (Fig. 1b), from the fibril-forming protein tau, associated with Alzheimer's disease²⁴. Again, microcrystals grown under different conditions (Ref 5, and see Methods) produced different structures related by a shift in registration of the two sheets. These two pairs of polymorphs, of segments SSTNVG and VQIVYK, show that a given fibril-forming sequence can form distinct steric zippers by adopting distinct registrations of the two β -sheets. We term this *registration polymorphism*.

Two additional pairs of steric zippers (Fig. 1c, d), one from the fibril-forming segment NNQQ of the yeast prion Sup35²¹, and the other from the segment NNQNTF of elk prion protein associated with strains²⁵, reveal what we term *facial polymorphism*. In the steric zippers on the right, the two sheets are packed face-to-face, as in the SSTNVG and VQIVYK. The steric zippers on the left are packed face-to-back (NNQQ), or back-to-back (NNQNTF).

Each of the eight steric zippers of Figure 1 appears stable and is likely separated from its alternative polymorph by a high energy barrier. Each β -sheet of a zipper is stabilized by main chain hydrogen bonds between layers. The two sheets of a zipper are held together by van der Waals bonds between the highly complementary, interdigitated side chains, and in a few cases by intersheet hydrogen bonds, as in the left polymorph of SSTNVG (Fig. 1a). To transform one polymorph into another, it is necessary to break the inter-sheet contacts, reposition the two sheets, and interdigitate the side chains to form the second zipper. The high energy barrier presented by bond breaking means that the two polymorphs are distinct, stable, long-lived structures.

Segmental polymorphism in steric zippers of IAPP

The amyloid-forming protein IAPP displays a rich variety of fibril morphologies^{11, 18}. Here we show that IAPP also displays a rich variety of steric zippers: six different segments of the IAPP sequence form distinct amyloid-like fibrils and microcrystals (Fig. 2). Instead of different packings of the same segment, described above, each of these polymorphic steric zippers is formed from a different segment of the IAPP sequence (Supplementary Figs. 2–4).

The six IAPP segments of Figure 2 form fibrils and needle-shaped microcrystals suitable for X-ray diffraction studies. Each of the six microcrystals reveals a distinctive steric zipper structure. We expect that fibrils and microcrystals formed by the same segment have similar structures, because: fibrils and microcrystals often grow under the same condition (see the micrograph of NNFGAIL fibrils, Fig. 2); in both, the extended segment is perpendicular to the long axis, with the β -sheets parallel to the axis; both give characteristic amyloid diffraction peaks at ~ 10 and 4.7 \AA ²⁶, and occasionally we find fibrils that appear to emanate from the tips of microcrystals (see the micrograph of HSSNNF fibrils, Fig. 2). In short, six segments of one protein, IAPP, form six fibril-like structures, each differing from all the others at the atomic level, a striking segmental polymorphism.

Full-length IAPP forms distinct steric zippers

Our biochemical studies of human and mouse IAPP (hIAPP and mIAPP, respectively) show that the spines of full-length IAPP fibrils can be built from steric zippers of at least two different segments. hIAPP forms fibrils of several morphologies^{11, 18}, whereas mIAPP does not form fibrils²⁷ (Fig. 3a). The established involvement of the C-terminal region (residues 21–37) in hIAPP fibrillization²⁸ is reinforced by differences in the human and mouse sequences (Fig. 2a and Supplementary Fig. 1); five of the six residue differences are in the C-terminal region.

We find that the N-terminal region of IAPP (residues 1–20) is also sufficient to drive fibrillization. Replacement of arginine 18 in mIAPP with histidine (mIAPP R18H), as in hIAPP, imparts fibril-forming ability to mIAPP, although these fibrils form more slowly than those of hIAPP²⁹ (Fig. 3a). Also, the pH profile of mIAPP R18H fibril formation shows an inflection at pH 6 (Supplementary Fig. 5), roughly the pKa of the substituted histidine, further implicating His18 in fibrillization (Fig. 3b). Clearly the C-terminal region of mIAPP R18H is not responsible for fibrillation because of the mouse substitutions that prevent fibrillation (Fig. 2a). Moreover, as shown in Figure 3c, the fibrils of hIAPP and mIAPP

R18H differ in morphology. A further experiment suggests that a segment within the C-terminus preferentially forms the spine within full-length human IAPP. In this experiment (Fig. 3a), substitution of the mouse residue into human IAPP at position 18 (H18R) does not affect the kinetics of fibril formation (Fig. 3a). It does, however, lower the fluorescence maximum, probably due to lower ThT binding, perhaps from alternative packing of protofibrils into fibrils.

Thus, the hIAPP sequence contains at least two fragments capable of forming amyloid cross- β spines: the C-terminal region, with a high propensity to form a zipper spine and a kinetically less favorable segment within the N-terminal region, containing His18 (Fig. 3a). The formation of a steric zipper within either region would preclude the formation of a steric zipper within the other region of the same molecule. Considering this result in light of the structures of Figure 2, suggests that full length IAPP can form polymorphs based on segmental polymorphism at the atomic level.

DISCUSSION

Peptide polymorphs, prion strains, and amyloid polymorphs

Our determination of molecular structures for polymorphic short segments falls far short of revealing the molecular structures for the entire polymorphic fibrils themselves. Solid state NMR, H/D exchange, cryoelectron microscopy, and other methods^{10–12, 14, 16, 18, 19, 30} have illuminated some fibrous molecular structures, but not yet atomic structures associated with strains. The highest resolution view to date of a prion fibril is that of HET-s³¹, in which the sidechains protruding from pairs of β -strands interdigitate, much like the sidechains within steric zippers. That the structures of full proteins in fibrils are more complicated than the structures of short segments is certain: amyloid proteins generally have more than a single segment that forms a steric zipper, and thus protein fibrils probably contain more than a single type of β -sheet. In fact, one strain might differ from another in part by the order in which the various steric zippers are nucleated. The variety of steric zippers formed by IAPP (Fig. 2) gives a glimpse of the complexity of fibrous states that even a small protein can exhibit. However, even before the complexity of prion strains is fully understood, the models for polymorphism reported here offer one basis for thinking about “conformations” of prion strains at the molecular level.

A similarity between the polymorphic segment structures reported here, and actual prion strains and amyloid polymorphs of full proteins, is that different “conformations” arise from different environmental conditions. For example, Tanaka et al.³² showed that different strains of Sup35-NM can be produced by incubation at different temperatures. Similarly, Petkova et al.¹⁰ showed that distinct polymorphs of Alzheimer’s β -amyloid fibrils can be produced by either agitating the dissolved precursor or not agitating. In our case, the polymorphs are produced under different solution conditions. In cells, different environmental conditions might arise from differential hydration, oxidative, or xenobiotic stress.

Lastly, the disruptive effect of proline scanning to fibrillation propensity is similar between peptide fibrils and full length amyloid and prions. When proline residues from the non-fibrillizing mouse IAPP sequence are substituted into these fibrillizing segments from human IAPP, the segments no longer form fibrils. Three segments with proline replacements were tested: PPTNVG, PPTNVGSNTY, and PVLPPY. None of these segments formed fibrils nor microcrystals over a period of a year. These observations strengthen the relevance of the short segments whose structures are presented here to the behavior of fibrils of the full protein.

Information transfer in biology

The results presented here suggest that the protein-encoded information transfer associated with prion strains shows similarities to nucleic acid-encoded information transfer of chromosomal inheritance (Table 3). The molecular basis for microbial strains is inherent in the central dogma of molecular biology: changes in gene sequence are translated into changes in protein structure; altered catalysis or interactions account for changed phenotypes of the mutant strains; and the phenotypes are heritable because the altered genes are inherited. In contrast, the prion hypothesis¹ – that a protein conformation can define a transmissible or heritable phenotype – was slow to be accepted, because the notion that multiple protein conformations can be heritable or transmissible fell outside common scientific experience. Proteins such as hemoglobin having alternative conformations have long been known. But the energy barriers between the conformations are low, and there was no known way that a conformation could be stabilized during the transmission to progeny cells. To achieve a high energy barrier between conformations there must be a strong non-covalent force that holds the protein in each distinctive conformation during the process of transmission.

The recognition that prion proteins can enter an amyloid-like, fibrillar state^{7, 33–35} offers a molecular mechanism for a stabilized, enduring conformation: the fibrillar state is maintained by a high density of hydrogen bonds³⁶. More recently we have found that amyloid and prion-derived fibrils have a steric-zipper spine maintained also by strong van der Waals forces between the sheets^{20, 21} and strong electrostatic polarization³⁷. The strong van der Waals forces bond self-complementary protein sequences, so that the interaction is sequence specific. Prion and amyloid-like fibrils are stable under physiological conditions, so that fibrils can be transmitted to progeny cells. Also, because a protein fibril introduced into a solution of the same protein can seed the dissolved molecules into fibrils, there is an evident molecular mechanism for prion conversion based on fibril properties³⁸.

Amyloid fibrils have the capacity for carrying the information of prion strains because they are polymorphic; the same protein can form a variety of distinct fibril types^{8–11, 14, 16, 30}. Yet the molecular mechanism of fibril polymorphism has remained obscure. One proposal, for the specific case of A β (1–40) fibrils, is that one polymorph is dimeric and the other trimeric¹⁶. But because prion strains and fibril morphologies are so varied^{6, 39}, there must be molecular mechanisms that are capable of encoding not just two polymorphs, but many.

The results of this paper suggest that the molecular basis of fibril polymorphism may be based on the large variety of steric-zipper amyloid spines that can form from a single protein. These mechanisms are summarized in Figure 4. Considering the possible variety of packing, segmental, and combined structures for steric zippers, it is clear that a substantial variety of prion strains associated with a single protein can be encoded by steric zippers. Although combinatorial polymorphism has not yet been observed on the atomic level, biochemical evidence suggests it may operate in Sup35 fibril polymorphism^{14, 15, 17}.

The molecular aspects of the transfer of genetic information by the familiar mechanism of nucleic acid inheritance show similarities to the less familiar protein-based mechanism suggested here for prion strains. In both cases, transfer is by non-covalent bonding. In nucleic acid inheritance, information transfer is achieved by base-pairing, involving complementary hydrogen bonding between bases. In the mechanisms proposed here for prion strains, information transfer is achieved largely by the steric fit (i.e. van der Waals bonding) of short, self-complementary amino acid sequences, with hydrogen bonding maintaining the zipper spine. Both mechanisms are sequence specific, based on nucleic acid sequences or on self-complementary protein sequences. In the prion/amyloid case, hydrogen bonds maintain the integrity of the spine, whereas in nucleic acids, covalent bonds maintain

the integrity of the backbone. The greater integrity of the covalent backbone of nucleic acids provides a more robust mechanism for ensuring the continuity of life. Though the variation possible in protein-encoded inheritance is small in comparison to that in genomic DNA, the number of possible steric zippers is enormous. Though less structurally robust and more restricted in information content, protein-based inheritance could allow more rapid response to environmental changes than Mendelian mechanisms⁴⁰. In short, the steric zipper presents an alternative model of information transfer which appears to have been adopted by a few microbial and mammalian proteins and perhaps many others, yet to be discovered⁴¹.

METHODS

Amyloid propensity prediction

We predicted fibril-formation propensities for human and mouse IAPP sequences using the 3D Profile method⁴². This algorithm uses the amyloid-like crystal structure of the NNQQNY segment²⁰ as a structural template. Each six-residue proline-free segment sequence is threaded onto the NNQQNY backbone structure, and the energetic fit is evaluated using the RosettaDesign program⁴³. Based on energies of experimentally determined amyloid-like segments, we chose an energy threshold for fibril-formation propensity of $-23 \text{ kcal mol}^{-1}$. That is, segments with computed energies equal to or below this threshold are deemed to have high propensity to form fibrils. The energies of all hexameric segments in IAPP were plotted, assigning the computed energy to the first residue of the hexameric segment (Fig. 2a).

Crystallization and Structure Determination

All peptide segments (custom synthesis, CS Bio) were crystallized using the hanging drop/vapor diffusion method. Details of crystallization, structure determination and refinement for each of the novel structures are provided in the Supplementary Information.

Fibril Formation

Lyophilized segments were dissolved to 1 mM in 100% hexafluoroisopropanol (HFIP), then diluted to 10 μM in 20 μM sodium acetate pH 6.5 (1% (v/v) HFIP final). Fibril formation was monitored by thioflavin T fluorescence at 450 nm excitation and 482 nm emission wavelengths. Data were collected in triplicate; error bars show the standard deviation between samples. For the experiments performed as a function of pH, samples were allowed to incubate at least one day and the final ThT fluorescence signal averaged for at least three samples is shown for comparison. The quiescent samples were incubated with 10 μM ThT at 37°C in various buffer conditions for appropriate pH. The measured presence or absence of fibrils was confirmed by negative stain electron microscopy (data not shown).

Supplementary Material

Refer to Web version on PubMed Central for supplementary material.

Acknowledgments

We thank the NE-CAT beamline at the APS for beamtime and collection assistance, and NSF, NIH, and HHMI for financial support.

References

1. Prusiner SB. Prions. *Proc Natl Acad Sci U S A*. 1998; 95:13363–83. [PubMed: 9811807]
2. Chien P, Weissman JS, DePace AH. Emerging principles of conformation-based prion inheritance. *Annu Rev Biochem*. 2004; 73:617–56. [PubMed: 15189155]

3. Wickner RB, Edskes HK, Shewmaker F, Nakayashiki T. Prions of fungi: inherited structures and biological roles. *Nat Rev Microbiol.* 2007; 5:611–8. [PubMed: 17632572]
4. Ross ED, Minton A, Wickner RB. Prion domains: sequences, structures and interactions. *Nat Cell Biol.* 2005; 7:1039–44. [PubMed: 16385730]
5. Collinge J, Sidle KC, Meads J, Ironside J, Hill AF. Molecular analysis of prion strain variation and the aetiology of ‘new variant’ CJD. *Nature.* 1996; 383:685–90. [PubMed: 8878476]
6. Legname G, et al. Continuum of prion protein structures enciphers a multitude of prion isolate-specified phenotypes. *Proc Natl Acad Sci U S A.* 2006; 103:19105–10. [PubMed: 17142317]
7. Caughey B, Chesebro B. Prion protein and the transmissible spongiform encephalopathies. *Trends Cell Biol.* 1997; 7:56–62. [PubMed: 17708907]
8. Tanaka M, Chien P, Naber N, Cooke R, Weissman JS. Conformational variations in an infectious protein determine prion strain differences. *Nature.* 2004; 428:323–8. [PubMed: 15029196]
9. King CY, Diaz-Avalos R. Protein-only transmission of three yeast prion strains. *Nature.* 2004; 428:319–23. [PubMed: 15029195]
10. Petkova AT, et al. Self-propagating, molecular-level polymorphism in Alzheimer’s β -amyloid fibrils. *Science.* 2005; 307:262–5. [PubMed: 15653506]
11. Goldsbury CS, et al. Polymorphic fibrillar assembly of human amylin. *J Struct Biol.* 1997; 119:17–27. [PubMed: 9216085]
12. Jones EM, Surewicz WK. Fibril conformation as the basis of species- and strain-dependent seeding specificity of mammalian prion amyloids. *Cell.* 2005; 121:63–72. [PubMed: 15820679]
13. Lundmark K, Westermark GT, Olsen A, Westermark P. Protein fibrils in nature can enhance amyloid protein A amyloidosis in mice: Cross-seeding as a disease mechanism. *Proc Natl Acad Sci U S A.* 2005; 102:6098–102. [PubMed: 15829582]
14. Krishnan R, Lindquist SL. Structural insights into a yeast prion illuminate nucleation and strain diversity. *Nature.* 2005; 435:765–72. [PubMed: 15944694]
15. Tessier PM, Lindquist S. Prion recognition elements govern nucleation, strain specificity and species barriers. *Nature.* 2007; 447:556–61. [PubMed: 17495929]
16. Paravastu AK, Leapman RD, Yau WM, Tycko R. Molecular structural basis for polymorphism in Alzheimer’s β -amyloid fibrils. *Proc Natl Acad Sci U S A.* 2008; 105:18349–54. [PubMed: 19015532]
17. Chang HY, Lin JY, Lee HC, Wang HL, King CY. Strain-specific sequences required for yeast [PSI⁺] prion propagation. *Proc Natl Acad Sci U S A.* 2008; 105:13345–50. [PubMed: 18757753]
18. Madine J, et al. Structural insights into the polymorphism of amyloid-like fibrils formed by region 20–29 of amylin revealed by solid-state NMR and X-ray fiber diffraction. *J Am Chem Soc.* 2008; 130:14990–5001. [PubMed: 18937465]
19. Sachse C, Fandrich M, Grigorieff N. Paired beta-sheet structure of an A β (1–40) amyloid fibril revealed by electron microscopy. *Proc Natl Acad Sci U S A.* 2008; 105:7462–6. [PubMed: 18483195]
20. Nelson R, et al. Structure of the cross- β spine of amyloid-like fibrils. *Nature.* 2005; 435:773–8. [PubMed: 15944695]
21. Sawaya MR, et al. Atomic structures of amyloid cross-beta spines reveal varied steric zippers. *Nature.* 2007; 447:453–7. [PubMed: 17468747]
22. Wiltzius JJ, et al. Atomic structure of the cross- β spine of islet amyloid polypeptide (amylin). *Protein Sci.* 2008; 17:1467–74. [PubMed: 18556473]
23. Hoppener JW, Ahren B, Lips CJ. Islet amyloid and type 2 diabetes mellitus. *N Engl J Med.* 2000; 343:411–9. [PubMed: 10933741]
24. von Bergen M, et al. Assembly of tau protein into Alzheimer paired helical filaments depends on a local sequence motif ((306)VQIVYK(311)) forming beta structure. *Proc Natl Acad Sci U S A.* 2000; 97:5129–34. [PubMed: 10805776]
25. Sigurdson CJ, et al. De novo generation of a transmissible spongiform encephalopathy by mouse transgenesis. *Proc Natl Acad Sci U S A.* 2009; 106:304–9. [PubMed: 19073920]
26. Sunde M, et al. Common core structure of amyloid fibrils by synchrotron X-ray diffraction. *J Mol Biol.* 1997; 273:729–39. [PubMed: 9356260]

27. Nishi M, Chan SJ, Nagamatsu S, Bell GI, Steiner DF. Conservation of the sequence of islet amyloid polypeptide in five mammals is consistent with its putative role as an islet hormone. *Proc Natl Acad Sci U S A*. 1989; 86:5738–42. [PubMed: 2668946]
28. Betsholtz C, et al. Sequence divergence in a specific region of islet amyloid polypeptide (IAPP) explains differences in islet amyloid formation between species. *FEBS Lett*. 1989; 251:261–4. [PubMed: 2666169]
29. Green J, et al. Full-length rat amylin forms fibrils following substitution of single residues from human amylin. *J Mol Biol*. 2003; 326:1147–56. [PubMed: 12589759]
30. Tanaka M, Collins SR, Toyama BH, Weissman JS. The physical basis of how prion conformations determine strain phenotypes. *Nature*. 2006; 442:585–9. [PubMed: 16810177]
31. Wasmer C, et al. Amyloid fibrils of the HET-s(218–289) prion form a beta solenoid with a triangular hydrophobic core. *Science*. 2008; 319:1523–6. [PubMed: 18339938]
32. Tanaka M, Chien P, Yonekura K, Weissman JS. Mechanism of cross-species prion transmission: an infectious conformation compatible with two highly divergent yeast prion proteins. *Cell*. 2005; 121:49–62. [PubMed: 15820678]
33. Prusiner SB, et al. Scrapie prions aggregate to form amyloid-like birefringent rods. *Cell*. 1983; 35:349–58. [PubMed: 6418385]

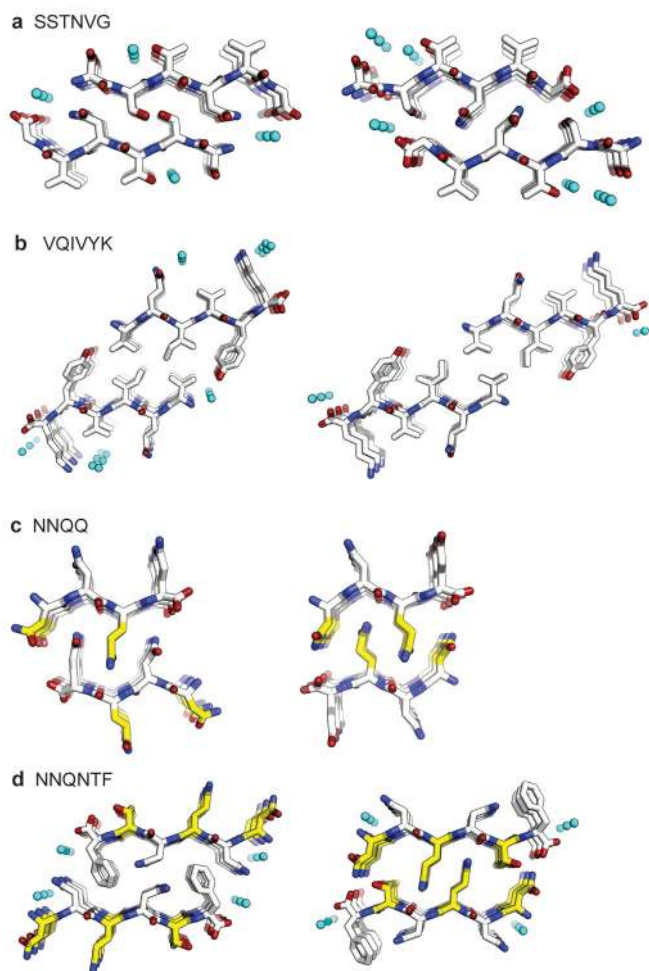


Figure 1.

Packing polymorphism of steric zippers, determined by X-ray microcrystallography. A steric zipper is a pair of interdigitated β -sheets, generally with a dry interface between them. The views here look down the fibril axes, showing three layers of the zipper. In actual fibrils and microcrystals, there are tens of thousands of layers. Each strand forms backbone hydrogen bonds to strands above and below it. Water molecules are shown as aqua spheres

a. Registration polymorphism of SSTNVG from islet amyloid polypeptide (IAPP). The left steric zipper (PDB code 3DG1²²) can be transformed to the right steric zipper by moving the top sheet to the left, and flipping side chains S2 and N4. **b.** Registration polymorphism of VQIVYK from tau protein. The left zipper (PDB code 2ON9²¹) can be transformed to the right zipper by moving the top sheet to the right. **c.** Facial polymorphism of NNQQ from yeast prion Sup35. The left NNQQ steric (PDB codes 2ONX²¹) zipper displays ‘face-to-back’ packing with N1 and Q3 amino acid side chains (yellow) of the top sheet interdigitated with Q4 and N2 (white) of the bottom sheet. In contrast, the right NNQQ steric zipper (PDB codes 2OLX²¹) displays ‘face-to-face’ packing, with N1 and Q3 side chains (yellow) of both sheets forming the interdigitated interface. **d.** Facial polymorphism of NNQNTF from elk prion protein²⁵. Both NNQNTF steric zippers are found in the same crystal structure, one face-to-face (right), with N1, Q3 and T5 (yellow) of both sheets forming the interdigitated interface; the other back-to-back, with sidechains N2, N4, and F6 interdigitated (white).

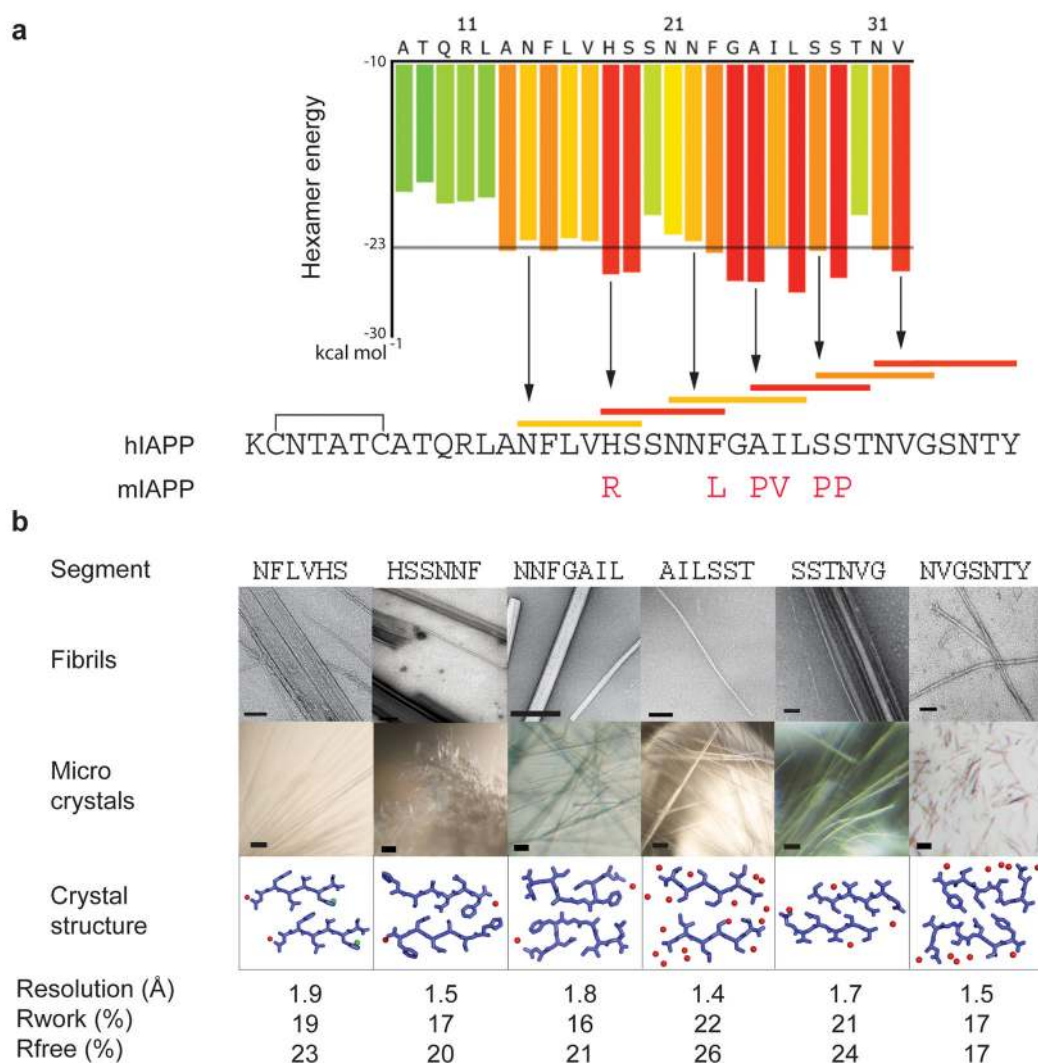


Figure 2. Segmental polymorphism in islet amyloid polypeptide (IAPP)

a. IAPP sequences and segment propensities for fibril formation. The sequence of human IAPP (hIAPP) is shown at bottom, with residue replacements in mouse IAPP (mIAPP) below. The histogram at top shows the estimated energies of steric zippers formed by six-residue segments (starting at the listed residue) of IAPP. Segments having energies of -23 kcal/mol or lower are predicted to form fibrils⁴². **b.** The six IAPP segments (highlighted with horizontal bars in **a**) were synthesized and found to form fibrils, as shown in the electron micrographs, top (scale bars are 100 nm). Each of the segments also forms microcrystals, shown in the light micrographs, upper middle (scale bars 50 μ m). The structures of the six segments were determined, lower middle, and each revealed a steric zipper. Resolutions and R-factors are given at the bottom; details are described in Supplementary Information. The electron micrographs of segments HSSNNF and NNFGAIL seem to show both microcrystals and fibrils.

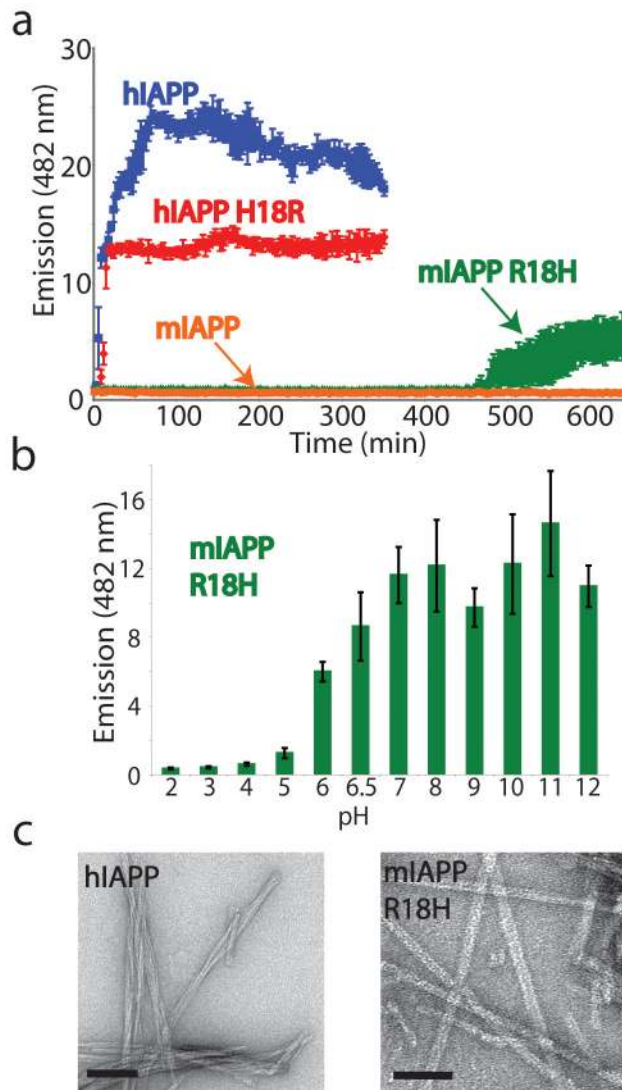


Figure 3. Evidence for at least two steric zipper polymorphs in full length IAPP

a. Mouse IAPP (mIAPP) does not form fibrils, in contrast to human IAPP (hIAPP) which rapidly forms fibrils. The mutation of R18 to H in mIAPP now permits mIAPP R18H to form fibrils. **b.** The pH dependence of mIAPP R18H fibrillization supports the involvement of His18. The error bars are the standard deviation of six replicates. **c.** hIAPP fibrils are commonly twisted and ~8 nm in width; mIAPP R18H fibrils are uniformly wider (~9–10 nm) and untwisted (scale bars are 50 nm), suggesting a different underlying structure.

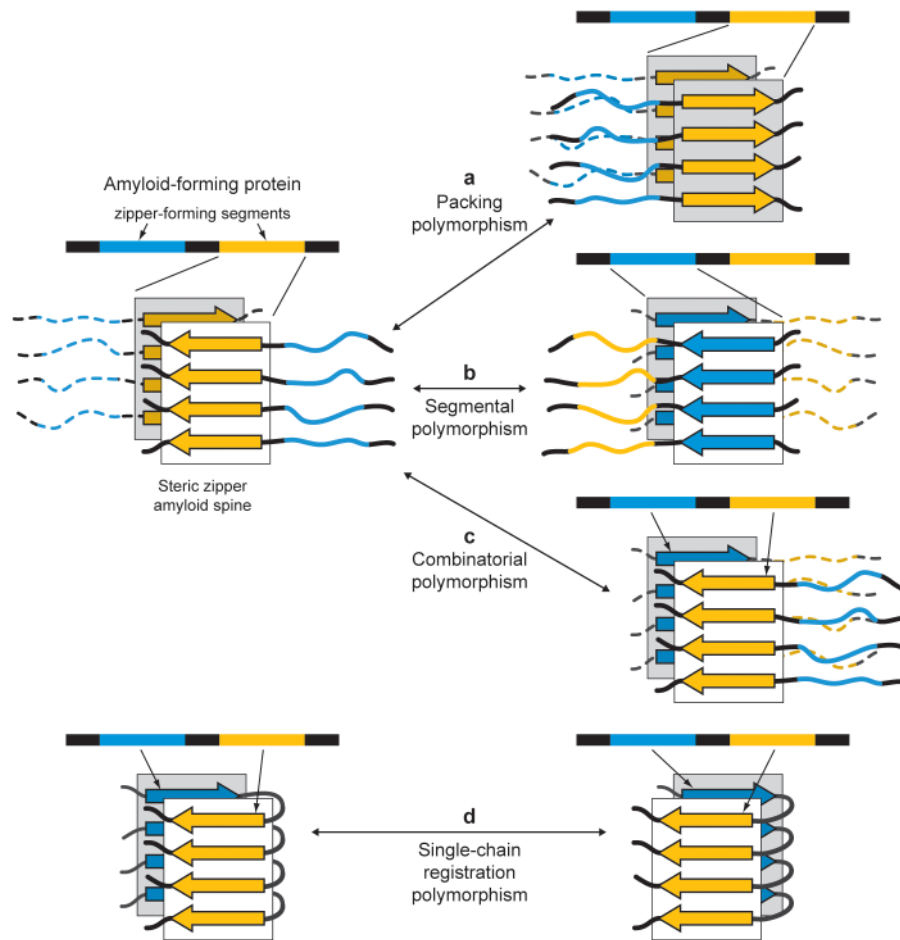


Figure 4. Schematic summary of steric-zipper mechanisms for amyloid and prion polymorphism
 On the left, an amyloid-forming protein is depicted with two segments (blue and yellow) each capable of forming a self-complementary steric zipper. Below the linear sequence is shown a steric zipper formed by the yellow segment with two β-sheets face-to-face. **a.** Packing polymorphism, in which the yellow segment has a sequence capable of forming a second steric zipper with the two β-sheets packing face-to-back as well as face-to-face. **b.** Segmental polymorphism, in which both the yellow and blue segments have sequences capable of forming self-complementary steric zippers. **c.** Combinatorial polymorphism, in which the blue and yellow segments have sequences capable of engaging in a steric zipper. **d.** Single-chain registration polymorphism, in which two segments of the same chain form two steric zippers with different registrations of their sidechains. Compare this to Figures 1a and 1b where the registration polymorphs are formed from identical segments of different chains. Neither combinatorial nor single-chain-registration polymorphisms have yet been observed at atomic resolution.

Table 1
 Statistics of data collection and refinement for new structures illustrated in Fig. 1

	SSTNYG Form 2	VQJYK Form 2	NNQNTF
Data collection			
Space group	P2 ₁ -2 ₁ -2 ₁	C2	P2 ₁
Cell dimensions			
<i>a</i> , <i>b</i> , <i>c</i> (Å)	16.59, 4.79, 40.23	28.64, 4.88, 35.81	18.06, 4.84, 21.36
α , β , γ (°)	90.0, 90.0, 90.0	90.0, 110.5, 90.0	90.0, 100.1, 90.0
Resolution (Å)	1.6	1.5	1.45
<i>R</i> _{merge} (%) (linear)	14.9 (49.9)	16.0 (37.6)	13.7 (27.3)
<i>I</i> / σ <i>I</i>	6.5 (1.3)	8.1 (4.7)	7.2 (3.4)
Completeness (%)	92.6 (85.7)	94.4(82.1)	98.7 (100.0)
Redundancy	4.5 (2.8)	4.1(4.0)	5.4 (4.3)
Refinement			
Resolution (Å)	20.11-1.61(1.80- 1.61)	33.54-1.51 (1.68-1.51)	21.0- 1.46 (1.46-1.50)
No. reflections	503 (78)	825(156)	707 (40)
<i>R</i> _{work} / <i>R</i> _{free}	22.3/25.3 (26.5/39.6)	17.4/19.6 (19.6/27.0)	16.2/17.4 (23.6/39.6)
No. atoms			
Protein	39	58	52
Ligand/ion	0	0	0
Water	3	1	2
<i>B</i> -factors			
Protein	8.6	6.8	0.7
Ligand/ion	-	-	-
Water	22.2	26.0	2.0
R.m.s. deviations			
Bond lengths (Å)	0.004	0.007	0.007
Bond angles (°)	0.91	1.03	0.77

* One crystal was used for each data set. Values in parentheses are for highest-resolution shell.

Table 2
 Statistics of data collection and refinement for new structures illustrated in Fig. 2

	NFLVHS	NFLVHSS	HSSNFF	AILSST	NVGSNTRY Form 1	NVGSNTRY Form 2
Data collection						
Space group	P2 ₁ -2 ₁ -2 ₁	P2 ₁	P2 ₁	P2 ₁	P2 ₁	P2 ₁
Cell dimensions						
<i>a</i> , <i>b</i> , <i>c</i> (Å)	9.55, 11.48, 38.58	9.73, 21.60, 26.09	4.82, 16.39, 23.48	9.54, 86.65, 19.48	20.63, 4.70, 21.01	20.65, 4.82, 29.05
α , β , γ (°)	90.0, 90.0, 90.0	90.0, 95.6, 90.0	90.0, 92.5, 90.0	90.0, 90.0, 90.0	90.0, 92.3, 90.0	90.0, 101.3, 90.0
Resolution (Å)	1.85	1.84	1.50	1.40	1.50	1.60
<i>R</i> _{merge} (%) (linear)	18.3 (41.9)	18.9 (46.0)	15.9 (57.2)	17.5 (55.9)	18.9 (39.2)	15.5 (49.0)
<i>I</i> / σ <i>I</i>	7.3 (2.5)	5.7 (2.2)	9.5 (3.7)	8.3 (2.0)	6.2 (2.2)	6.6 (2.7)
Completeness (%)	93.9 (82.9)	95.2 (89.1)	93.6 (75.6)	84.5 (85.5)	95.0 (86.5)	95.7 (94.0)
Redundancy	5.4 (6.4)	2.8 (2.8)	4.3 (4.4)	2.7 (2.5)	5.2 (2.8)	3.1 (3.1)
Refinement						
Resolution (Å)	19.29-1.85 (1.90- 1.85)	25.97-1.84 (1.89- 1.84)	23.45-1.50 (1.68- 1.50)	43.31-1.40 (1.44- 1.40)	20.99-1.50 (1.67- 1.50)	28.51-1.60 (1.78- 1.60)
No. reflections	379	825	509	4723	662	984
<i>R</i> _{work} / <i>R</i> _{free}	19.2/23.2 (29.5/26.9)	23.8/28.2 (25.5/21.6)	17.3/20.7 (20.4/21.2)	22.2/26.5 (30.8/34.9)	14.8/15.8 (19.9/27.7)	12.4/15.9 (17.8/23.1)
No. atoms						
Protein	51	124	50	328	53	318
Ligand/ion	1	5	0	0	0	0
Water	1	7	4	67	5	0
B-factors						
Protein	13.5	6.7	4.2	11.8	3.9	2.5
Ligand/ion	69.9	33.1	-	-	-	-
Water	32.7	17.2	20.4	24.3	7.1	-
R.m.s. deviations						
Bond lengths (Å)	0.005	0.016	0.004	0.003	0.006	0.009
Bond angles (°)	0.61	1.56	0.70	0.79	1.12	1.66

* Four crystals were used for NVGSNTY form 1. Two crystals were used for NFLVHSS. One crystal was used for each of the remaining data sets. Values in parentheses are for highest-resolution shell.

Table 3

A comparison of molecular mechanisms of inheritance

	<u>Nucleic acid encoded</u>	<u>Protein encoded</u>
Encoding elements	DNA or RNA sequence	Steric zipper structure
Sequence dependent?	Yes	Yes
Recognition by	Base pairing	Amino acid sidechain complementarity
Backbone stability	Covalent sugar-phosphate	High density hydrogen bonding
Information content	Virtually unlimited	Potentially large
Adaptive advantages	High stability and information content	Rapid adaptation to environmental changes